Elsevier Editorial System(tm) for
Electrochimica Acta

Manuscript Draft

Manuscript Number: EA18-2960

Title: HIGHLY EFFICIENT PLASMONIC DYE-SENSITIZED SOLAR CELLS WITH SILVER NANOWIRES AND TiO2 NANOFIBRES INCORPORATED MULTI-LAYERED PHOTOANODE

Article Type: Research Paper

Keywords: Dye sensitized solar cells, efficiency enhancement, Silver nanowires, plasmonic effect, tri-layered photoanode, TiO2 nanofibers

Corresponding Author: Professor Malavi A.K.L. Dissanayake, Ph.D.

Corresponding Author's Institution: Institute of Fundamental Studies

First Author: Malavi A.K.L. Dissanayake, Ph.D.

Order of Authors: Malavi A.K.L. Dissanayake, Ph.D.; Mihirangi G Kumari, BSc; C S Perera, BSc, PhD; Buddhika S Dassanayake, BSc, MS, PhD; G K Senadeera, BSc, PhD

Abstract: In this study, the effect of incorporating silver nanowires (Ag NWs) and TiO2 nanofibers (NFs) into a tri-layer photoanode of dye sensitized solar cells (DSSCs) have been investigated. Ag NWs with diameter 60-90 nm and length of 1-2 µm were synthesized via polyol reduction method. TiO2 nanofibers (NFs) with diameter 80-120 nm were prepared by electrospinning.
The DSSC with tri-layer photoanode made with composite TiO2 P25, Ag NWs and TiO2 NFs sandwiched between two TiO2 P25 layers exhibited power conversion efficiency (PCE) of 9.74% and open circuit voltage (Voc), short circuit current density (Jsc) and fill factor (FF) of 727.4 mV, 19.8 mA cm-2 and 67.6% respectively under the irradiance of 100 mW cm-2. The efficiency of the reference DSSC with TiO2 P25/P25/P25 tri-layer photoanode of the same thickness was found to be 6.69%. The efficiency enhancement of the DSSC with Ag NW and TiO2 NF incorporated composite, tri-layer photoanode compared to the reference DSSC is 45.6%. This is evidently due to the enhancement in short-circuit photocurrent density (Jsc) by (a) localized surface plasmon resonance effect by Ag NWs and (b) increased light harvesting by multiple scattering events by the presence of TiO2 NFs.

National Institute of Fundamental Studies
Kandy, Sri Lanka

E-mail: makldis@yahoo.com Tel: +94 81 2232002 Fax: +94 81 2232131

8th May 2018

Prof. A.R. Hillman
Editor in Chief, Electrochimica Acta
Dept. of Chemistry,
University of Leicester,
University Road,
LE1 7RH, Leicester,
UK

Dear Professor Hillman,

Submission of a research article to be published in Electrochimica Acta

I wish to submit the following original research article, titled:
Highly efficient plasmonic dye-sensitized solar cells with silver nanowires and TiO_2 nanofibres incorporated multi-layered photoanode
co-authored by M.G.C.M.Kumari, C.S. Perera, B.S. Dassanayake, M.A.K.L. Dissanayake, and G.K.R. Senadeera to your esteemed journal, **Electrochemica Acta.**

This article is based on our original research work at the National Institute of Fundamental Studies, Kandy, Sri Lanka (http://nifs.ac.lk/).

To the best of our knowledge, this is the first report of the use of a multilayer TiO_2 photoanode structure consisting of a composite of TiO_2 P25 nnoparticles, TiO_2 Nanofibre and Ag nano wires in a DSSC exhibiting a remarkable efficiency enhancement of 45.6% with respect to a TiO2 P25 Photoanode of the same thickness.

I would appreciate very much if you could please consider publishing this article in your esteemed journal Electrochimica Acta.
Sincerely yours,

M.A.K.L. Dissanayake

B.Sc. (Ceylon)., M.S. Ph.D. (Indiana, Bloomington, USA),
D.Sc. (Wayamba, Sri Lanka)
Research Professor, NIFS

Suggested Reviwers

1.. Prof. K. Ramesh, Department of Physics, University of Malaya, Kula Lumpur, Malaysia.

E-mail: rameshkasi@um.edu.my

2.. Prof. B.-E. Mellander, Department of Applied Physics, Chalmers University of Technology, Gothenburg, SWEDEN.
E-mail: f5xrk@chalmers.se

3.. Prof. Ajit Kulkarni, Department of Meterials Eng. IIT, Bombay, India

E-mail: ajit.kulkarni@iitb.ac.in

Submitted to Electrochimica Acta 8th May 2018
Corr. Author: M.A.K.L. Dissanayake

HIGHLY EFFICIENT PLASMONIC DYE-SENSITIZED SOLAR CELLS WITH SILVER NANOWIRES AND TiO_2 NANOFIBRES INCORPORATED MULTI-LAYERED PHOTOANODE

M.G.C.M.Kumari[1], C.S. Perera[1], B.S. Dassanayake[1], M.A.K.L. Dissanayake[2*] and G.K.R. Senadeera [2,3]

[1]Department of Physics, University of Peradeniya, Peradeniya, Sri Lanka
[2]National Institute of Fundamental Studies, Kandy, Sri Lanka.
[3]Department of Physics, The Open University of Sri Lanka, Nawala, Nugegoda, Sri Lanka

[*]Corresponding Author, e-mail: *makldis@yahoo.com*

ABSTRACT

In this study, the effect of incorporating silver nanowires (Ag NWs) and TiO_2 nanofibers (NFs) into a tri-layer photoanode of dye sensitized solar cells (DSSCs) have been investigated. Ag NWs with diameter 60-90 nm and length of 1-2 µm were synthesized via polyol reduction method. TiO_2 nanofibers (NFs) with diameter 80-120 nm were prepared by electrospinning.

The DSSC with tri-layer photoanode made with composite TiO_2 P25, Ag NWs and TiO_2 NFs sandwiched between two TiO_2 P25 layers exhibited power conversion efficiency (PCE) of 9.74% and open circuit voltage (V_{oc}), short circuit current density (J_{sc}) and fill factor (FF) of 727.4 mV, 19.8 mA cm^{-2} and 67.6% respectively under the irradiance of 100 mW cm^{-2}. The efficiency of the reference DSSC with TiO_2 P25/P25/P25 tri-layer photoanode of the same thickness was found to be 6.69%. The efficiency enhancement of the DSSC with Ag NW and TiO_2 NF incorporated composite, tri-layer photoanode compared to the reference DSSC is 45.6%. This is evidently due to the enhancement in short-circuit photocurrent density (J_{sc}) by (a) localized surface plasmon resonance effect by Ag NWs and (b) increased light harvesting by multiple scattering events by the presence of TiO_2 NFs.

Keywords: Dye sensitized solar cells, efficiency enhancement, Silver nanowires, plasmonic effect, tri-layered photoanode, TiO_2 nanofibers

1. INTRODUCTION

The conventional DSSC is a device generally consisting of a mesoporous layer of TiO_2 nanoparticles with a monolayer of Ruthenium dye adsorbed on the TiO_2 nanoparticle surfaces, a liquid or quasi-solid (gel) electrolyte with iodide/triiodide redox couple and a platinized counter electrode. Since the first report of the DSSC by Gratzel et al in 1991 [1], it is under intense research in order to develop low cost, stable and high performance solar cells. These were mainly achieved by developing better photoanodes [2-4], novel sensitizers [5,6] and novel electrolytes [7-11].

The dye adsorbed photoanode is one of the key components of a DSSC which determines the efficiency of it. The efficiency of a device can be substantially enhance either by increasing the thickness of the photoanode and hence the increase in dye adsorption or fabricating photoanodes with suitable structural modifications [1,2]. However, increase of the film thickness is not that simple due to various reasons such as poor adherence to the substrate, formation of cracks, reduction of light penetration etc. [12]. Therefore, most of the investigations are carried out on the structural modifications of the photoanode. For example by incooperatrion of TiO_2 nanofibers (NFs), Nanotubes, Nano wires (NWs) or nano flakes in to the photoanode [13-19].

Light trapping or scattering techniques can also be used effectively to improve the performance of the photoanodes which could enhance the short circuit photocurrent and hence the efficiency of a DSSC. Strategically designed and nanostructurally developed, smart light trapping techniques can be used to obtain 'optically thick' light absorbers to allow substantially enhanced light absorption [20]. Generally this light trapping or scattering is achieved by using a scattering layer with bigger size nanoparticle layer (~ 300-700 nm) depositing on top of a smaller size nano particle (~ 20 nm) layer [21,22].

Recently it has been also explored that, incorporating TiO_2 nanofibers (NFs) to the photoanode is another way to increase the optical thickness of the photoanode. TiO_2 NFs can trap more light by scattering the incoming light. Mie scattering theory successfully explains the light scattering by TiO_2 NFs [23]. Here the "optical thickness" of the photoanode is increased due to the tailoring of the photoanode composition and the geometry either by using NFs or NWs in the structure of the photoanode [24-33]. In order to further enhance the overall performance of DSSCs, strategically increasing the short circuit photocurrent density by nanostructural modifications to the photoanode could be implemented. By

tailoring the photoanode composition, and geometry with 1-D nanostructures such as TiO_2 NWs and TiO_2 NFs, improvements in electron mobility and transport have been observed [26-36].

In recent studies, it was observed that localized surface plasmon resonance (LSPR) effect can also be utilized in the photovoltaics devices [37]. When an electromagnetic (EM) wave is incident on a metal surface, due to the electric field component of EM wave, there will be collective oscillations of the surface conduction electrons or surface plasmons. As metal nanostructures have sub wavelength dimensions, oscillation of electron cloud (plasma) is localized/confined around the surface of the nanostructure resulting LSPR effect [38]. There are mainly four light enhancement types contributing to generation of photoelectrons via LSPR effect in DSSC photoanodes; (1) near field coupling of electromagnetic fields, (2) far-field coupling of scattered light (3) plasmon resonance energy transfer and (4) hot electron transfer [39-43]. Silver is a noble metal showing strong LSPR effects [43,44]. Thus by incorporating Ag NWs to photoanode of a DSSC, an enhancement in DSSC performance originating from the increase in the photocurrent has been achieved [44-,47].

In this study, DSSCs made with tri-layered TiO_2 photoanodes consisting of a composite made of a TiO_2 nano-particle (NP) layer with Ag NWs and TiO_2 NFs sandwiched between two TiO_2 NP layers were fabricated and characterized. A liquid phase bottom-up polyol reduction synthesis method was used to chemically synthesis Ag NWs. Electrospinning method was used to fabricate of TiO_2 NFs. To the best of our knowledge, this is the first report of the use of a tri-layer TiO_2 photoanode structure consisting of a composite of TiO_2 P25 nnoparticles , TiO_2 Nanofibre and Ag nano wires in a DSSC.

2. EXPERIMENTAL

2.1 Synthesis of silver nanowires (Ag NWs)

2.1.1 Materials

For the synthesis of Ag NWs, Silver nitrate ($AgNO_3$, 99.8%, Daejung), polyvinyl pyrrolidone (PVP, Mw = 44,000, BOH Laboratories), Glycerol (Surechem Products LTD), sodium chloride (NaCl, 99.5%, Sigma-Aldrich) were used as received without any further purification. The deionized (DI) water was used from the Millipore system.

2.1.2 Synthesis of Ag NWs

The Ag NWs were synthesized using polyol reduction process published elsewhere [44]. First, 47.5 ml of glycerol and then 1.500 g of PVP were added to a round bottom flask. Then, the solution was gently heated up to 80 °C until all PVP was dissolved. The solution was then cooled down to room temperature and 0.395 g of $AgNO_3$ powder was added to the solution. Subsequently, 0.125 ml of NaCl solution (5 mmol/L) was added to 2.5 ml of glycerol and the latter was added to the PVP dissolved solution containing $AgNO_3$ powder. Next, the reaction temperature of the solution was increased rapidly to 210 °C, roughly at a rate of 8 °C per min. while stirring in a magnetic stirrer at 50 rpm under aerobic condition. When the temperature reached 210 °C the heating was stopped and the solution was allowed to cool down to room temperature. Then 50 ml of DI water was added to the flask and the mixture was centrifuged at 8000 rpm for 20 minutes and Ag NWs were collected. Finally, in order to remove the residues including PVP, nano wires were washed with copious amount of DI water by centrifuging the suspension.

2.1.3 Characterization of Ag NWs

In order to study the optical properties of the synthesized Ag NWs, a suspension of nanowires was prepared with DI water and UV-visible absorption spectrum of it was obtained using a Shimadzu UV-1800 spectrometer. The dimensions and the morphology of the Ag NWs were studied using a scanning electron microscope(SEM) (EVO LS15).

2.2 Synthesis of TiO_2 NFs

2.2.1 Materials

Poly (vinyl acetate) (PVA, $(C_4H_6O_2)n$), titanium isopropoxide (TIP, $C_{12}H_{28}O_4Ti$, Fluka Chemie, Switzerland) and acetic acid (99 %, Fisher), N,N-dimethylforamide (DMF, Degussa) were used as starting materials to synthesize TiO_2 NFs.

2.2.2 Preparation of TiO_2 NFs

A mixture containing 1.5 g polyvinyl acetate (PVA), 3 g Titanium (iv) isopropoxide (TIP) and 1.2 g of Acetic acid as a catalyst for sol-gel reaction in 19 ml of N,N-dimethylforamide (DMF) was magnetically stirred for 6 hours. Then, the solution was electrospun to obtain TiO_2 nanofibres (NF) under a voltage of 15 kV applied between the syringe needle tip and the

grounded drum collector. The distance between the nozzle and collector was kept as 6.5 cm. The drum was rotated with a rotational speed of 650 rpm. The electrospun TiO_2 NFs were deposited on pre cleaned glass plates. Finally, the electrospun NFs were calcined at 450 °C for 45 min.

2.2.3 Characterization of TiO_2 NFs

The dimensions and the morphology of the Ag NWs were studied using a scanning electron microscope (EVO LS15).

2.3 Fabrication of DSSC

2.3.1 Fabrication of pristine TiO_2 nanoparticle (TiO_2-NP) photoanode

In one of our previous studies, we have optimized the film thickness of the TiO_2 nanoparticle layer suitable for DSSCs [37]. However in that study we have fabricated the TiO_2 nanoparticle films as a single layer and optimum efficiency was obtained with a ~ 12.73 μm thick film. Further increase of the thickness of the TiO_2 film resulted in a decrease of the efficiency of the DSSC and it was difficult to fabricate thicker films due to poor adherence to the FTO substrate. Therefore, by considering these factors in this study we have fabricated thicker photoanodes by separately forming the three layered photo anodes with pristine TiO_2 with optimized total thickness of about 28 μm. Further improvements to the adherence and the reduction of short-circuiting were achieved by applying a pinhole free compact layer on the FTO substrate [47].

At first a thin, compact layer (CL) of TiO_2 was spin coated for one minute at 3000 rpm on pre-cleaned Fluorine doped tin oxide glass substrate (FTO) (Solaronix sheet glass 7 Ω/sq) by using a paste prepared by grinding 0.250 g TiO_2 (Aeroxide P-90) with 1.0 ml of 0.1 M HNO_3 for 15 min. The solution was spin coated on pre-cleaned FTO glass substrate (Solaronix sheet glass 7 Ω/sq) at 3000 rpm for 60 s, followed by sintering at 450 °C for 45 min. After cooled downed to room temperature, on top of the compact layer, single layer of mesoporous TiO_2 ~~layer~~ was fabricated as follows. First, 0.250 g of TiO_2 powder (Desgussa P-25) was ground for 30 min with 1.0 ml of 0.1M HNO_3, one drop of Triton X-100 and 0.050 g of PEG. The paste was then deposited on top of the compact layer by "doctor blading" method, followed by sintering at 450 °C for 45 min. After cooling down to room temperature another layer of

TiO_2 NP was deposited on top of the above layer and followed the same sintering procedure. Finally third layer of P25 NP was applied on top of the above double layered structure by following the same procedure. After cooled down to room temperature, these glass substrates with tri- layered TiO_2 NP films were dipped in an ethanolic dye (0.3 mM) solution containing Ruthenium dye N719 [RuL2 (NCS)2:2TBA where, L = 2,2'-bipyridyl-4,4'-dicarboxylic acid TBA = tetrabutylammonium] for 24 h . The effective area of the photoanodes was kept 0.25 cm^2. The film thickness estimated from SEM analysis was ~ 28 μm. In order to compare the efficiencies of DSSCs , dye adsorption was also carried out for the single layered (~ 12.73 μm) TiO_2 NPs films as in the other cases.

2.3.2 Preparation of Ag NWs incorporated photoanodes

Efficiency optimization of DSSCs having different amounts of AgNWs were carried out in one of our previous studies [47]. It was found that 2.2% (wt %) of NWs with respect to TiO_2 weight gives the highest efficiency. Therefore in this study Ag NWs incorporated photoanodes were prepared by using the same weight ratio. Appropriate amount of AgNws were added to the TiO_2 paste prepared for the doctor blade method and ground well the mixture and films were fabricated by Doctor blade method. TiO_2 films with Ag NWs were heat treated at 450 ^oC for 45 minutes and after cooled it down to room temperature dye adsorption also carried out as above.

2.3.3 Preparation of TiO_2 NFs incorporated photoanodes

Similar to optimization of photoanode composition by incorporating Ag NWs [47] , DSSCs having different amounts of TiO_2 NFs in their photoanodes were fabricated. The optimized DSSC efficiency was achieved by mixing 95% TiO_2 (P 25) powder (0.2375 g) with 5% electrospun TiO_2 NF powder (0.0125 g).

2.3.4 Preparation of the redox electrolyte

The redox electrolyte solution containing I^-/I_3^- was prepared by adding a 3.6 ml of molten (MP 40 $^\circ C$) ethylene carbonate (EC) and 1.0 ml of acetonitrile to a pre-cleaned 10 ml volumetric flask. Then the solution was stirred overnight, after adding a 0.738 g of tetrapropyl ammonium iodide (Pr_4NI) and 0.060 g of I_2 to the volumetric flask.

2.3.5 Fabrication of solar cells and their I-V characterization

In order to compare the performances of DSSCs several types of solar cells consisting with dye adsorbed (a) FTO/P90/P25NP/P25NP/P25NP tri-layered (b) FTO/P90/P25NP/(P25NP+AgNWs)/P25NP, (c) FTO/P90/P25NP/(P25NP+TiO_2 NFs)/P25NP and (d) FTO/P90/P25NP/(P25 +Ag NWs + TiO_2 NFs) /P25NP, photoanodes were prepared by sandwiching them individually with Pt coated FTO glass counter electrodes together with the above electrolyte . The total thickness of each of the above (a), (b), (c) and (d) photo-anodes were kept nearly the same at ~ 28 µm.

The photocurrent-voltage (I-V) characteristics of the prepared DSSCs were measured under the simulated sunlight illuminating at 100 mW cm^{-2} (AM 1.5). A Xenon 500 W lamp with AM 1.5 filter was used as the solar simulator to obtain the above intensity. The solar simulator was coupled with a Keithley 2000 multimeter and a potentiostat/galvanostat HA-301.

2.3.6 EIS measurements on DSSCs

Electrochemical Impedance Spectroscopy (EIS) measurements were performed on the above four DSSCs using a Metrohm Autolab Potentiostat/Galvanostat PGSTAT 128 N with a FRA 32 M Frequency Response Analyzer (FRA) covering the 1 MHz-0.01 Hz frequency range. These measurements were carried out under the illumination of 1000 Wm^{-2} simulated sunlight using the same solar simulator that was used for *I-V* measurements.

3. RESULTS AND DISCUSSION

3.1 Single layer DSSC

Figure 1 shows the SEM image of the cross section of the mesoporous single layer TiO_2 (P25NP) photoanode incorporating Ag NWs. It should be mentioned here that single layer TiO_2 films of larger thickness than what is shown in Fig. 1 could not be formed by the doctor blade method with good adhesion to the FTO substrate and without cracking during sintering. Whether it is pure TiO_2 (P25NP) or Ag NW incorporated TiO_2, 12.73 µm is about the maximum film thickness that could be formed without cracking [37,47]. However, thicker,

crack-free TiO_2 photoanode films could be formed by doctor blading followed by sintering layer by layer. Therefore, The tri-layer TiO_2 P25NP/P25NP/P25NP photoanodes with compact P90 TiO_2 layer used in this work have been prepared by this method.

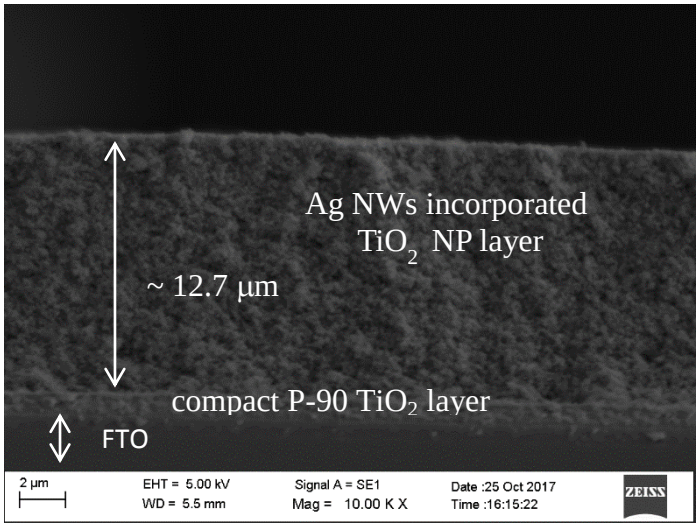

Fig. 1: SEM image of the Ag NWs incorporated single -layered TiO_2 photoanode.

SEM images of the top view of the synthesized Ag NWs and electro spun TiO_2 NFs are shown in Figure 2. As seen from these images, the average dimensions of the synthesized Ag NWs are 2.5 µm in length and 78 nm in diameter. The average diameter of the TiO_2 NFs is 115 nm.

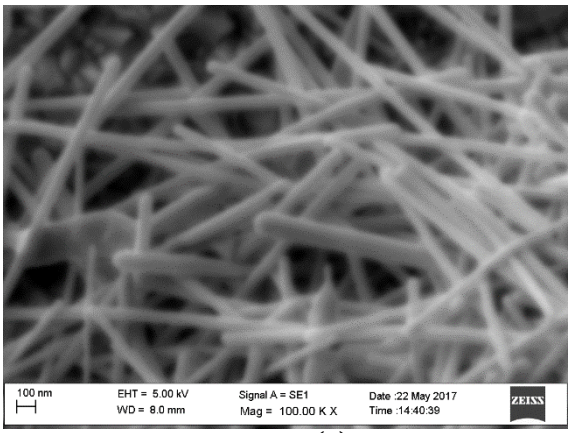

(a)

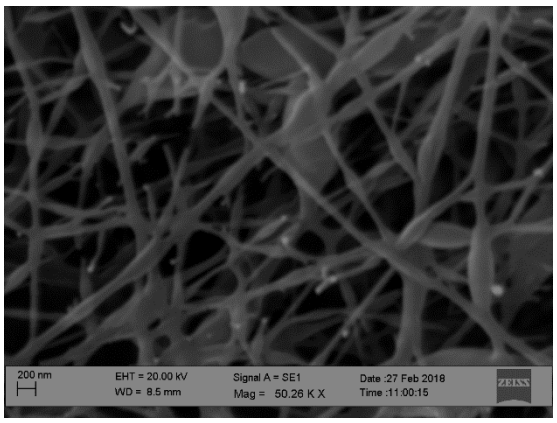

(b)

Fig. 2: SEM images of (a) synthesized Ag NWs and (b) electro spun TiO_2 NFs

3.2 DSSCs with tri-layer phtoanodes

The optimization of single layer thickness of pristine TiO_2 (P-25) photoanode of DSSC has been reported previously by our group and published elsewhere [37]. The DSSCs fabricated with a TiO_2 photoanode of ~ 12.73 μm thickness have shown the best photovoltaic performance with highest incident photon-to-current conversion efficiency and highest short-circuit photocurrent. Although thicker TiO_2 single layer photoanodes were expected to have better photovoltaic performance, these could not be fabricated due to the development of cracking and peeling off the TiO_2 film due to poor adherence. However, by depositing one layer at a time followed by sintering, it was possible to make thicker TiO_2 photoanodes and these were optimized for the best solar cell performance of total tri-layer thickness of about 28 μm. Having a thicker multilayer pristine TiO_2 photoanode as the reference is useful when the effects of different inner layers on the photovoltaic performance of DSSCs are studied.

SEM images show that the total thickness of the optimized tri-layer photoanode is ~ 28 μm and the thickness of each TiO_2 layer is around 8.00-10.00 μm. This is the same for all four different types of photoanodes tested here, viz. a) FTO/P90/P25NP/P25NP/P25NP tri-layered with TiO_2 P25NP as the middle layer, (b) FTO/P90/P25NP/(P25NP+AgNWs)/P25NP, with the P25NP mixed with TiO_2 NF as the middle layer, (c) FTO/P90/P25NP/(P25NP+TiO_2 NFs)/P25NP, mixed with Ag NWs as the middle layer and (d) FTO/P90/P25NP/(P25 +Ag NWs + TiO_2 NFs) /P25NP, with TiO_2 NFs and Ag NWs as the middle layer.

One of the SEM images of the tri-layered photoanode, FTO/P90/P25NP/**(**P25NP+Ag NW+TiO_2 NF)/P25NP, is presented in Figure 3 as a representative example. The composite middle layer consists of one of the compositions, (P25NP+TiO_2NF) or (P25NP+Ag NW) or (P25NP+Ag NW+TiO_2 NF) in optimized composition ratios. Fig. 3(b) shows a schematic diagram of the DSSC with the tri-layer photoanode (d) P25/P25+Ag NW+TiO_2 NF/P25.

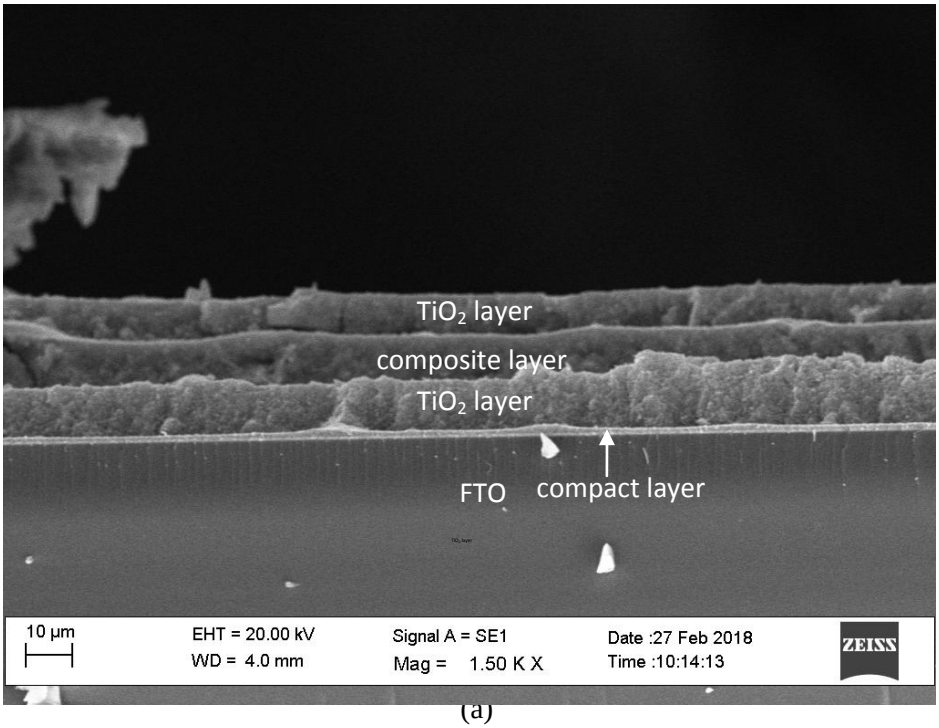

(a)

Fig.3 (a): SEM image of TiO_2 photoanode of the tri-layered structure; P25/P25+Ag NW+TiO_2 NF/P25 formed on FTO/P-90 compact layer correspond to the DSSC showing the best photovoltaic performance. The composite middle layer consists of the optimized composition of P25+Ag NW+TiO_2 NF.

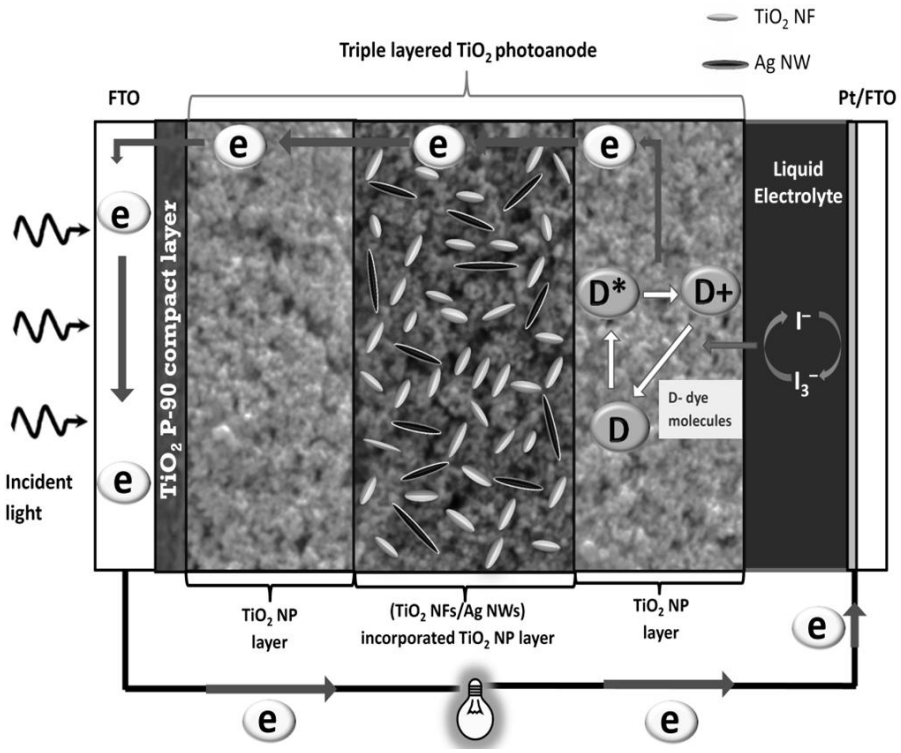

(b)

Fig. 3(b) : A schematic diagram of the DSSC with the tri-layer photoanode (d) P25/P25+Ag NW+TiO_2 NF/P25.

3.2.1 Photovoltaic performance

The photovoltaic performance of the DSSCs with above four different types of tri-layered photoanodes measured under the simulated sunlight illuminating at 100 m W cm^{-2} (AM 1.5) are shown as *J-V* curves in Fig.4.

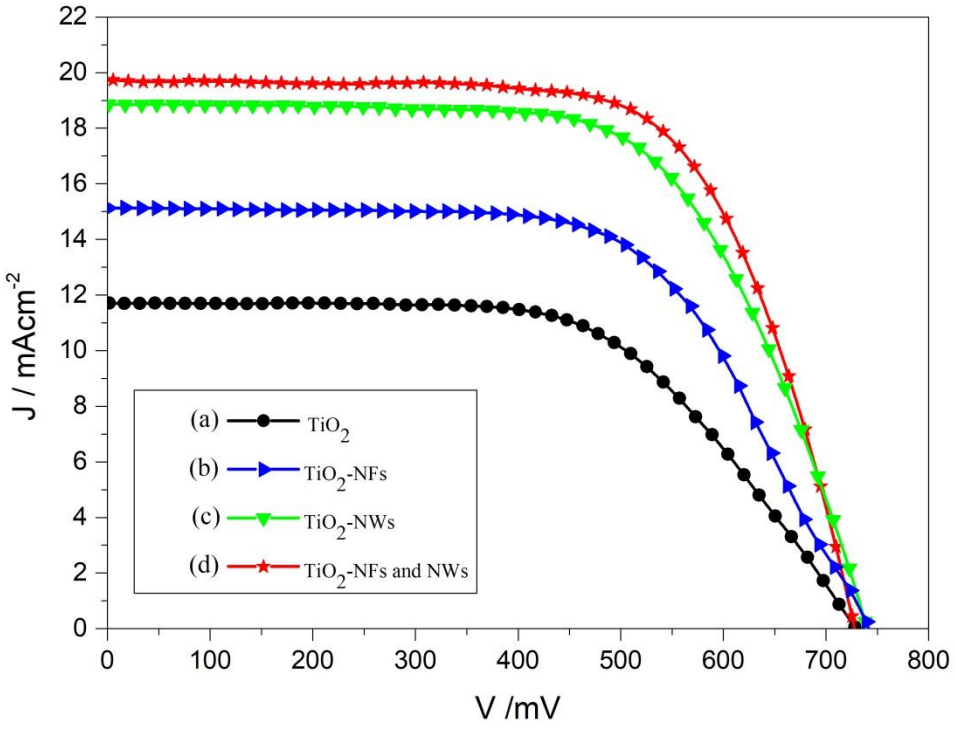

Fig 4: *J-V* curves taken for DSSCs with tri-layer photoanodes (a) P25NP/P25NP/P25NP tri-layer with TiO_2 P25NP as the middle layer, (b) P25NP/(P25NP+TiO_2 NFs)/P25NP, with the P25NP mixed with TiO_2 NF as the middle layer, (c) P25NP/(P25NP+AgNWs)/P25NP, with the P25NP mixed with AgNW as the middle layer and (d) P25NP/(P25 +Ag NWs + TiO_2 NFs) /P25NP, with the P25NP mixed with TiO_2 NFs and Ag NWs as the middle layer.

The corresponding photovoltaic parameters derived from above the photocurrent density-voltage measurements are tabulated in Table 1.

Table 1. Photovoltaic parameters of the DSSCs with tri-layer photoanodes (a) FTO/P90/P25NP/P25NP/P25NP (b) FTO/P90/P25NP/(P25NP+AgNWs)/P25NP, (c) FTO/P90/P25NP/(P25NP+TiO_2 NFs)/P25NP, and (d) FTO/P90/P25NP/(P25 +Ag NWs + TiO_2 NFs) /P25NP.

Tri-layered photoanode configuration with compact P90 layer	J_{sc} **(mAcm^{-2})**	V_{oc} **(mV)**	*FF* **(%)**	η **(%)**
(a) P25NP/(*P25NP)*/P25NP (reference)	14.3	746.9	62.6	6.69
(b) P25NP/(P25NP+TiO_2 NF) /P25NP	15.8	729.7	70.0	8.07
(c) P25NP/(P25NP+Ag NW)/P25NP	18.9	741.9	62.7	8.94
(d) P25NP/(P25NP+Ag NW+TiO_2NF)/P25NP	19.8	727.4	67.6	9.74

From a comparison of the performance of the DSSCs with four different composite, three layered photoanodes (a), (b), (c) and (d) shown in Figure 5 and Table 1, the results of improved short circuit photocurrenet and the enhanced efficiency of the DSSCs with modified photoanodes can be interpreted as follows;

The increased photocurrent density and the efficiency when the TiO_2 P-25NP middle layer is replaced by a mixture of TiO_2 P25 NP and TiO_2 NF (from photoanode (a) to photoanode (b)), is evidently due to the improved light harvesting due to presence of the TiO_2 nanofibres in the middle layer. This is very likely due to the increased light absorption caused by multiple scattering effects in the TiO_2 nanofibre based photoanode as already reported by us and by others [24-28]. As a result, the J_{sc} has increased by 10.5% and the efficiency by 20.6%. In a previous paper we have described in detail, somewhat qualitatively, how multiple light scattering events contribute to the enhancement of light harvesting within the TiO_2 nanofibre structure consisting of "elongated bead" shaped short nanofibres formed after sintering [26,28].

Multiple scattering events by elongated nanofibre beads within the sintered NF layer coupled with possible back and forth reflections from the two interfaces on either side of middle layer of the TiO_2 photoanode appears to contribute to this enhancement.

Zhu et al has reported that the efficiency enhancement in their DSSCs made with "rice grain shaped" TiO_2 nanobeads is due to improved light harvesting by scattering [24]. Similar improvement in light harvesting by scattering by a composite TiO_2 electrode consisting of a mixture of nanofibres and nanoparticles has been discussed in detail by Joshi et al. [25]. These authors have attributed the enhancement in efficiency to the enhanced photocurrent due to improved light harvesting through Mie scattering. According to their results, under the same fabrication conditions and with the same TiO_2 photoanode film thickness, the DSSCs made from the composite with 85 wt% nanoparticles and 15 wt % nanofibers have showed a 44% higher efficiency compared to those made from TiO_2 nanoparticles alone.

In line with these already published reports, we can infer that the enhancement in the photocurrent and the efficiency of the DSSCs with tri-layer photoanode (b) P25NP/(P25NP+TiO_2 NF) /P25NP where the middle layer consists of a mixture of TiO_2 nanoparticles (95 wt%) and TiO_2 nanofibres (5 wt%) used in our work is evidently due to the scattering enhanced photocurrent due to the presence of the optimized nanoparticle-nanofibre ("*elongated beads*") composite middle layer sandwiched between the two TiO_2 P25NP layers.

As explained in several papers mentioned in the introduction section, the localized surface plasmon resonance (LSPR) effect is very likely responsible for the observed enhancement in the photocurrent and the efficiency in the DSSCs with tri-layer photoanode, (c) (P25NP/**(***P25NP+Ag NW)***/**P25NP where the middle layer consists of the optimized mixture of TiO_2 P25NP and Ag NWs [37-45]. The increase in J_{sc} and efficiency is more prominent here compared to the photoanode (b) made with TiO_2 NFs in the middle layer. The photocurrent density has increased by 32% and the efficiency by 33.6% with respect to the pristine photoanode (a) P25NP/P25NP/P25NP.

When the middle layer is replaced by the optimized mixture of TiO_2 P25NP powder, together with ~~electrospun and~~ sintered electrospun TiO_2 nanofibres (TiO_2 NF) and silver nanowires (Ag NWs), i.e ~~and~~ the change of the photoanode structure from (a) P25NP/*P25NP*/P25NP) to (d) (P25NP/**(***P25NP+Ag NW+*TiO_2 *NF)/* P25NP) the increase in J_{sc} and efficiency is much more prominent. The photocurrent density has increased by 38.5% and the overall efficiency by 45.6% with respect to the basic (reference) DSSC with pristine P25NP/*P25NP*/P25NP photoanode of the same thickness. The cumulative effect of both, "scattering enhanced photocurrent" due to TiO_2 NFs as well as the "plasmon enhanced photocurrent" due to Ag Ns are evidently responsible for this remarkable photocurrent and efficiency enhancement. To the best of our knowledge, the use of a tri-layer TiO_2 photoanode structure consisting of a

composite of TiO_2 P25 nnoparticles , TiO_2 Nanofibre and Ag nano wires has not been used to achieve efficiency enhancement in a DSSC.

3.2.2 EIS analysis

Electrochemical impedance spectroscopy was performed in order to understand the electronic and ionic processes in DSSCs [34]. Nyquist plots and the Bode Plots in the frequency range from $11 \times 10^{-2}$to 1×10^{6} Hz taken for the DSSCs with photoanode configurations (on FTO/TiO2 compact layer) (a) P25/*P25*/P25) and (d) (P25/*P25+Ag NW+*TiO_2 *NF/* P25) are shown in Figures 5 and 6 respectively. The corresponding parameters extracted from the equivalent circuit analysis and Bode plots are tabulated in Table 2.

In each Nyquist plot, the larger semicircle in the low frequency range corresponds to the charge transport/accumulation at dye-attached TiO_2/electrolyte interface with resistance ($R2_{CT}$) and the smaller semicircle in the high frequency range corresponds to the charge-transfer resistance of the Pt counter electrode/electrolyte interface ($R1_{CT}$) [34]. The equivalent circuit for these Nyquist plots is also shown in Figure 5. Impedance parameters $R1_{CT}$ and $R2_{CT}$ along with series resistance R_s of the two DSSCs can be execrated from these equivalent circuits.

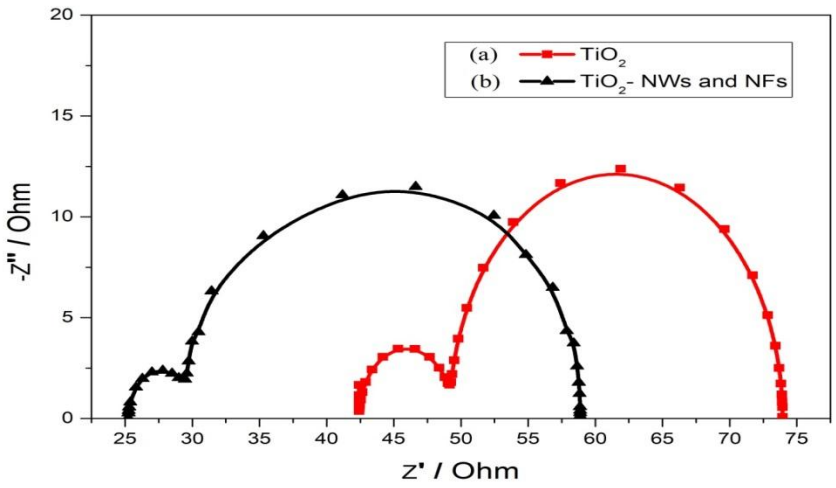

Fig.5 Impedance plots taken for the DSSCs with photoanodes with configurations (a) (P25/P25/P25) and (b) (P25/P25+Ag NW+TiO_2 NF/P25) in the frequency range 11×10^{-2} to 1×10^{6} Hz.

The Bode phase plots of EIS spectra are shown in Figure 7. In a Bode phase plot complex impedance data are plotted as phase angle vs. frequency [48]. A Bode phase plot shows frequency peaks of the charge transfer process at the TiO_2/electrolyte interface. The characteristic frequency peak for the reference DSSC with pristine photoanode, (a) (P25NP\P25NP\P25NP) and the DSSC with (b) (P25NP\(P25+Ag NW+TiO_2 NF)\P25NP) composite photoanode are 8.~~69 8.6851~~ Hz and 12.65 ~~12.649~~ Hz respectively. It is clear that the characteristic frequency peak (f_{max}) has been shifted to a lower frequency when Ag NWs and TiO_2 NFs are incorporated into the middle layer of the photoanode. From f_{max} value the electron lifetimes (τ_e) can be obtained using the following equation [48],

$$f_{max} = \frac{1}{2\pi\tau_e}$$

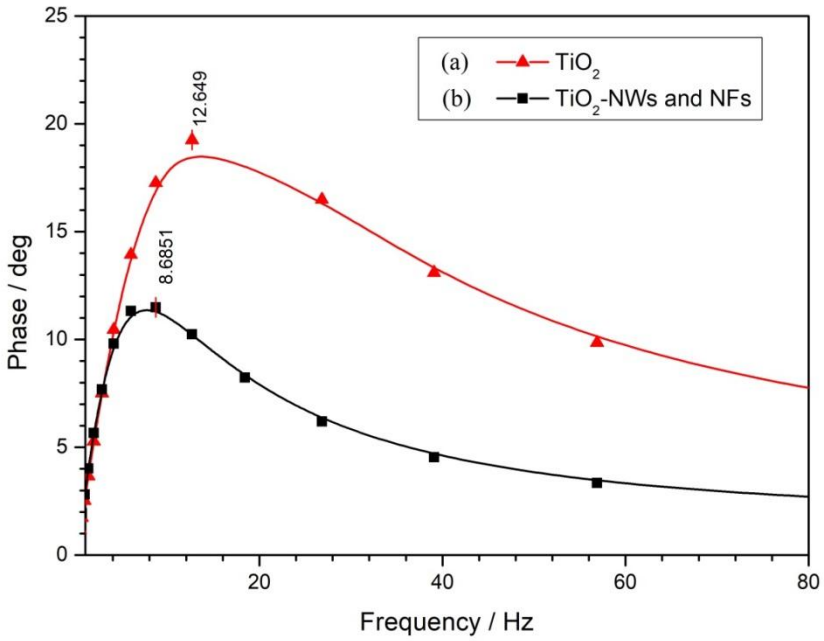

Fig.6. Bode phase plots taken for the DSSCs with photoanodes with configurations (a) (P25/P25/P25) and (b) (P25/P25+Ag NW+TiO_2 NF/P25) in the frequency range 11×10^{-2} to 1×10^{6} Hz.

The impedance parameters $R1_{CT}$, $R2_{CT}$, f_{max} along with the photovoltaic parameters and τ_e extracted from EIS measurements are tabulated in Table 2.

Table 2 charge-transfer resistance of the Pt/electrolyte ($R1_{CT}$), charge-transfer resistances of the TiO_2/electrolyte ($R2_{CT}$), characteristic frequency peak (f_{max}) and electron recombination life times (τ_e), along with photovoltaic parameters of DSSCs with photoanodes (a) (P25NP/*P25NP*/P25NP) and (d) (P25NP/(*P25NP+Ag NW+TiO_2 NF*)/P25NP configured on FTO/TiO_2 CL.

DSSC TiO_2 Photoanode Configuration	**PCE (%)**	**J_{sc} (mAcm^{-2})**	***$R1_{CT}$* (Ω)**	***$R2_{CT}$* (Ω)**	**f_{max} (Hz)**	**τ_e (ms)**
(a)P25NP/*P25NP*/P25NP (reference)	6.69	14.3	15.3	7.89	8.6851	18.3
(d)P25NP /(*P25NP+Ag NW+TiO_2 NF*)/P25NP	9.74	19.8	7.56	4.32	12.649	12.6

As seen from Table 2, there is a decrease in $R1_{CT}$ and $R2_{CT}$ values for the DSSC with composite photoanode (d) P25/P25+AgNW+TiO_2NF/P25 compared to the DSSC with reference photoanode (a) P25/P25/P25. The decrease in $R1_{CT}$ implies that the increase in the oxidation rate and the redox mediator favours the electron collection at the Pt counter electrode [48,49]. The decrease in the resistance value of $R2_{CT}$ with respect to the reference cell suggests that the incorporation of Ag NWs has improved the charge transfer process across the composite photoanode (d) and the electrolyte. This is very likely due to the better Ag NWs mediated conductivity. The improvement in electron transfer process at TiO_2 /electrolyte interface contributes to the overall improvement in the electron transfer process in the photoanode. The decrease in $R2_{CT}$ also implies that the electrons released by the redox couple reach the oxidized dye molecule easily.

From Table 2, it is evident that the electron lifetime is highest for the DSSC with composite photoanode (d) P25NP/*(P25NP+Ag NW+TiO_2 NF*)/P25NP ~~Ag NWs~~ . This means that in this photoanode, electrons diffuse and transfer more easily. Higher electron lifetime also implies reduced recombination of photoelectrons between TiO_2 photoanode and the electrolyte, which contributes to the enhancement in J_{sc} leading to overall efficiency enhancement.

4. CONCLUSION

In this work, the effect of incorporating Ag NWs and TiO_2 NFs into tri-layered photoanode of the DSSC has been investigated. By incorporating Ag NWs and TiO_2 NFs (with the optimized concentrations for single mesoporous TiO_2 layer) only to the middle layer of the photoanode, the efficiency enhancement is 45.6 % with respect to reference tri- layered DSSC with same thickness (~28 µm). The efficiency enhancement is mainly due to increased short circuit current density which can be attributed to the increase in photocurrent due to (a) LSPR effect of Ag NWs and (b) improved light harvesting by mutltiple scattering effects due to the presence of TiO_2 NFs in the middle layer of the tri- layered structure of the photoanode.

5. ACKNOWLEDGEMENT

The authors gratefully acknowledge the support from University of Peradeniya, Peradeniya, Sri Lanka and National Institute of Fundamental Studies (NIFS), Kandy, Sri Lanka. This investigation received financial support from the NSF under the Grant No NSF/PDRS/2017/01 .

REFERENCES

[1] B. O'Regan, M. Gra¨tzel, A low-cost, high-efficiency solar cell based on dye-sensitized colloidal TiO_2 films, Nature 353 (1991) 737-740.

[2] K. Hara, H. Arakawa, Dye-sensitized solar cells. In: Tachibana Y, Hara K, Sayama K, Arakawa H (Eds), Handbook of photovoltaic science and engineering. John Wiley & Sons Ltd, Chichester 2010, p. 664–670

[3] N. Koumura, Z. Wang, S. Mori, M. Miyashita, E. Suzuki, K. Hara, Alkyl-functionalized organic dyes for efficient molecular photovoltaics, J Am Chem Soc 128 (2006) 14256-14257.

[4] M. Gra¨tzel, Solar energy conversion by Dye-sensitized photovoltaic cells, Inorg Chem 44 (2005) 6841-6851.

[5] M. A. K. L. Dissanayake, C. A. Thotawatthage, G. K. R. Senadeera, T. M. W. J. Bandara, W. J. M. J. S. R Jayasundera, B. E. Mellander, Efficiency enhancement by mixed cation effect in dye-sensitized solar cells with PAN based gel polymer electrolyte, J Photochem Photobiol A 246 (2012) 29-35.

[6] H. Wang, X. Zhang, F. Gong, G. Zhou, Z. Wang, Novel ester functionalized solid-state electrolyte for highly efficient all-solid state dye-sensitized solar cells, Adv Mater 24 (2012) 121-124.

[7] M. A. K. L. Dissanayake, W. N. S. Rupasinghe, V. A. Seneviratne, C. A. Thotawatthage, G. K. R. Senadeera, Optimization of iodide ion conductivity and nano filler effect for efficiency enhancement in polyethylene oxide (PEO) based dye sensitized solar cells, Electrochim Acta 145 (2014) 319-326.

[8] M. Nazeeruddin, A. Kay, I. Rodicie, R. Humphry-Baker, E. Mu¨ller, P. Liska, Conversion of light to electricity by cis-XzBis(2,20-bipyridyl-4,40-dicarboxylate)ruthenium(11) charge transfer sensitizers (X = C1-, Br-, I-, CN-, and SCN-) on nanocrystalline TiO_2 electrodes, J Am Chem Soc 115 (1993) 6382-6390.

[9] M. A. K. L. Dissanayake, H. K. D. M. N. R. Divarathne, C. A. Thotawatthage, C. B. Dissanayake, G. K. R. Senadeera, B. M. R. Bandara, Dyesensitized solar cells based on electrospun polyacrylonitrile (PAN) nanofibre membrane gel electrolyte, Electrochim Acta 130 (2014) 76-81.

[10] How light trapping surfaces will boost solar cell efficiency [online] Available from: https://www.technologyreview.com/s/510016/how-light-trapping-surfaces-will-boost-solar-cell efficiency/ [Accessed 22nd October, 2017].

[11] K. Marchuk, K. A. Willets, Localized surface plasmons and hot electrons, Chemical Physics. Invited Perspective 445 (2014) 95-104.

[12] D. M. Schaadt, B. Feng, E. T. Yu, Enhanced semiconductor optical absorption via surface plasmon excitation in metal nanoparticles, Appl. Phys. Lett. 86 (2005) 063106 (http://dx.doi.org/10.1063/1.1855423).

[13] M. Ihara, K. Tanaka, K. Sakaki, I. Honma, K. Yamada, Enhancement of the Absorption Coefficient of cis-$(NCS)_2$ Bis(2,2‘-bipyridyl-4,4‘-dicarboxylate)ruthenium(II) Dye in Dye-Sensitized Solar Cells by a Silver Island Film, J. Phys. Chem. B 101 (1997) 5153-5157.

[14] M. K. Gangishetty, K. E. Lee, R. W. Scott, T. L. Kelly, Plasmonic Enhancement of Dye Sensitized Solar Cells in the Red-to-near-Infrared Region using Triangular Core–Shell $Ag@SiO_2$ Nanoparticles, ACS Appl. Mater. Interfaces 5 (2013) 11044-11051.

[15] S. K. Cushing, J. Li, F. Meng, T. R. Senty, S. Suri, M. Zhi, M. Li, A. D. Bristow, N. Wu, Photocatalytic activity enhanced by plasmonic resonant energy transfer from metal to semiconductor, J. Am. Chem. Soc. 134 (2012) 15033-15041.

[16] P. J. Schuck, Nanoimaging: Hot electrons go through the barrier, Nat. Nanotechnol. 8 (2013) 799-800.

[17] C. Yang, Y. Tang, Z. Su, Z. Zhang, C. Fang, Preparation of Silver Nanowires via a Rapid, Scalable and Green Pathway, Journal of Materials Science & Technology 31 (2015) 16-22.

[18] E. V. Ferry, J. N. Munday, H. A. Atwater, Design considerations for plasmonic photovoltaics, Adv. Mater. 22 (2010) 4794-4808.

[19] M. A. K. L. Dissanayake, J. M. K. W .Kumari, G. K. R. Senadeera, C.A. Thotawatthage, Efficiency enhancement in plasmonic dye-sensitized solar cells with TiO_2 photoanodes incorporating gold and silver nanoparticles, J Appl Electrochem 46 (2016) 47-58.

[20] M. G. C. M. Kumari, C. S. Perera, B. S. Dassanayake, M. A. K. L. Dissanayake, G. R. K. Senadeera, plasmon enhanced dye sensitized solar cell performance using TiO_2/Ag NW nanocomposite photoanode, in: Proc. Solar Asia 2018 International Conference, Kandy, Sri Lanka, 4-6 January 2018, p 179-184. (http://nifs.ac.lk).

[21] H. Xu, X. Chen, S. Ouyang, T. Kako, J. Ye, Size-Dependent Mie's Scattering Effect on TiO_2 Spheres for the Superior Photoactivity of H_2 Evolution**,** *J. Phys. Chem. C* 116 (2012) 3833-3839.

[22] P. Zhu, A. S. Nair, S. Yang, S. Peng, S. Ramakrishna, Which is a superior material for scattering layer in dye-sensitized solar cells-electrospun rice grain- or nanofiber-shaped TiO_2?, J. Mater. Chem. 21 (2011) 12210-12212.

[23] P. Joshi, L. Zhang, D. Davoux, Z. Zhu, D. Galipeau, H. Fong, Q. Qiao, Composite of TiO_2 nanofibers and nanoparticles for dye-sensitized solar cells with significantly improved efficiency, Energy Environ. Sci. 3 (2010) 1507.

[24] M. A. K. L. Dissanayake, H .K. D. W. M. N. Divarathnaa, C. B. Dissanayake, G. K. R. Senadeera, P. M. P. C. Ekanayakea, C. A. Thotawattage, An innovative TiO_2 nanoparticle/nanofibre/nanoparticle, three layer composite photoanode for efficiency enhancement in dye-sensitized solar cells, Journal of Photochemistry and Photobiology A: Chemistry 322 (2016) 110-118.

[25] M. A. K. L. Dissanayake, T. Jaseetharan, G. K. R. Senadeera, C.A. Thotawatthage, A novel, PbS:Hg quantum dot-sensitized, highly efficient solar cell structure with triple layered TiO_2 photoanode, Electrochimica Acta 269 (2018) 172-179.

[26] H. J. Koo, J. Park, B. Yoo, K. Kim, N. G. Park, Size-dependent scattering efficiency in dye-sensitized solar cell, Inorg. Chim. Acta 361 (2008) 677-683.

[27] G. K. Mor, K. Shankar, M. Paulose, O. K. Varghese, C. A. Grimes, Use of Highly-Ordered TiO_2 Nanotube Arrays in Dye-Sensitized Solar Cells, Nano Lett. 6 (2006) 215-218.

[28] V. Tan, Y. Y. J. Wu, Dye-Sensitized Solar Cells Based on Anatase TiO_2 Nanoparticle/Nanowire Composites, Phys. Chem. B 110 (2006) 15932-15938.

[29] Y. Ohsaki, N. Masaki, T. Kitamura, Y. Wada , T. Okamoto, T. Sekino, K. Niihara, S. Yanagida, Phys. Chem. Dye-sensitized TiO_2 nanotube solar cells: fabrication and electronic characterization, Chem. Phys. 7 (2005) 4157-4163.

[30] M. Law, L. E. Greene, J. C. Johnson, R. Saykally, P. D. Yang, Nanowire dye-sensitized solar cells, Nat. Mater. 4 (2005) 455-459.

[31] H. Kokubo, B. Ding, T. Naka, H. Tsuchihira, S. Shiratori, Multi-core cable-like TiO_2 nanofibrous membranes for dye-sensitized solar cells, Nanotechnology 18 (2007) 165604.

[32] M. Y. Song, Y. R. Ahn, S. M. Jo, D. Y. Kim, J. P. Ahn, Effects of down conversion luminescent film in dye-sensitized solar cells, Appl. Phys. Lett. 87 (2005) 113113.

[33] M. A. M. Ziyan, M. A. K. L. Dissanayake, U. L. Zainudeen, G. K. R. Senadeera, C.A. Thotawatthage, Study of dye-sensitized solar cells with TiO_2 nanoparticles/nanofibers composite electrode using photovoltic and EIS measurements, in: Proc.Solar Asia 2018 International Conference, Kandy, Sri Lanka, 4-6 January 2018, p-163-168 (http://nifs.ac.lk).

[34] Q. Wang, J. Moser, M. Gra1tzel, Electrochemical Impedance Spectroscopic Analysis of Dye-Sensitized Solar Cells, *J. Phys. Chem. B* 109 (2005) 14945–14953.

[35] H. Hoppe, N. S. Sariciftci, Organic solar cells: an overview, Journal of Materials Research 19 (2004) 1924-1945.

[36] J. M. K. W. Kumari, N. Sanjeevadharshini, M. A. K. L. Dissanayake, G. K. R. Senadeera, C. A. Thotawatthage, The effect of TiO_2 photoanode film thickness on photovoltaic properties of dye-sensitized solar cells, Ceylon Journal of Science 45 (2016) 33-41 (DOI: http://dx.doi.org/10.4038/cjs.v45i1.7362).

Submitted to Electrochimica Acta 8th May 2018
Corr. Author: M.A.K.L. Dissanayake

TABLES

Table 1. Photovoltaic parameters of the DSSCs with tri-layer photoanodes (a) FTO/P90/P25NP/P25NP/P25NP (b) FTO/P90/P25NP/(P25NP+AgNWs)/P25NP, (c) FTO/P90/P25NP/(P25NP+TiO_2 NFs)/P25NP, and (d) FTO/P90/P25NP/(P25 +Ag NWs + TiO_2 NFs) /P25NP.

Tri-layered photoanode configuration with compact P90 layer	J_{sc} **(mAcm^{-2})**	V_{oc} **(mV)**	***FF*** **(%)**	η **(%)**
(a) P25NP/(*P25NP)*/P25NP (reference)	14.3	746.9	62.6	6.69
(b) P25NP/(P25NP+TiO_2 NF) /P25NP	15.8	729.7	70.0	8.07
(c) P25NP/(P25NP+Ag NW)/P25NP	18.9	741.9	62.7	8.94
(d) P25NP/(P25NP+Ag NW+TiO_2NF)/P25NP	19.8	727.4	67.6	9.74

Table 2 charge-transfer resistance of the Pt/electrolyte ($R1_{CT}$), charge-transfer resistances of the TiO_2/electrolyte ($R2_{CT}$), characteristic frequency peak (f_{max}) and electron recombination life times (τ_e), along with photovoltaic parameters of DSSCs with photoanodes (a) (P25NP/*P25NP*/P25NP) and (d) (P25NP/(*P25NP+Ag NW+*TiO_2 *NF*)/P25NP configured on FTO/TiO_2 CL.

DSSC TiO_2 Photoanode Configuration	**PCE (%)**	J_{sc} **(mAcm^{-2})**	$R1_{CT}$ **(Ω)**	$R2_{CT}$ **(Ω)**	f_{max} **(Hz)**	τ_e **(ms)**
(a)P25NP/*P25NP*/P25NP (reference)	6.69	14.3	15.3	7.89	8.6851	18.3
(d)P25NP /(*P25NP+Ag NW+*TiO_2 *NF*)/P25NP	9.74	19.8	7.56	4.32	12.649	12.6

Submitted to Electrochimica Acta 8th May 2018
Corr. Author: M.A.K.L. Dissanayake

HIGHLY EFFICIENT PLASMONIC DYE-SENSITIZED SOLAR CELLS WITH SILVER NANOWIRES AND TiO_2 NANOFIBRES INCORPORATED MULTI-LAYERED PHOTOANODE

FIGURES with Captions

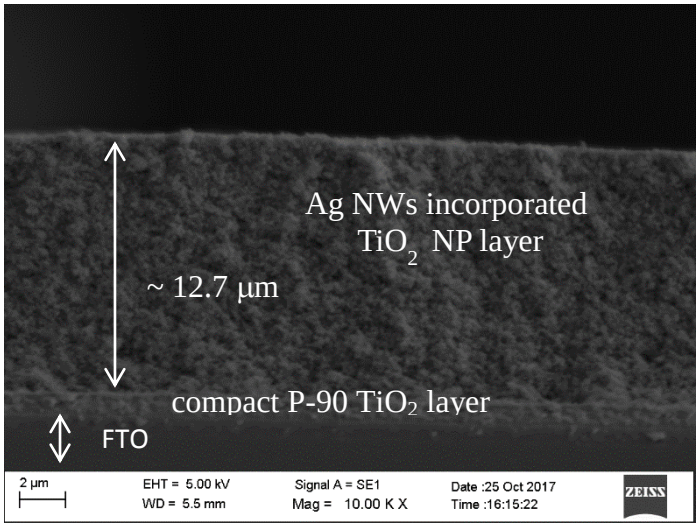

Fig. 1: SEM cross section image of the Ag NWs incorporated single -layered TiO_2 photoanode.

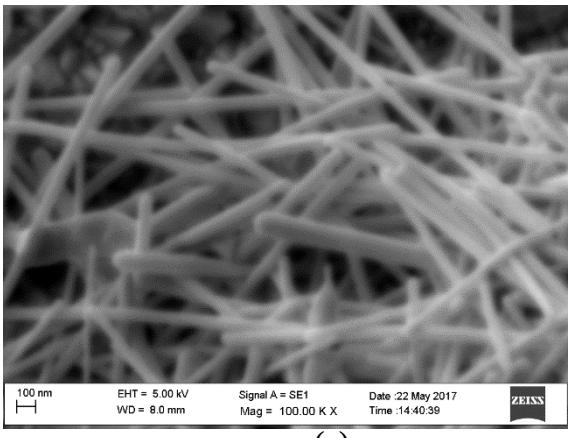

(a)

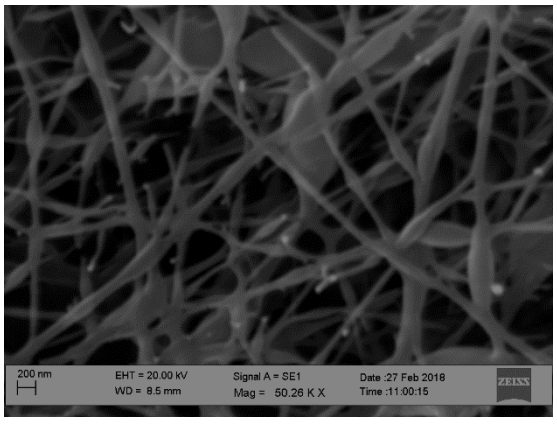

(b)

Fig. 2: SEM top view images of (a) synthesized Ag NWs and (b) electro spun TiO_2 NFs

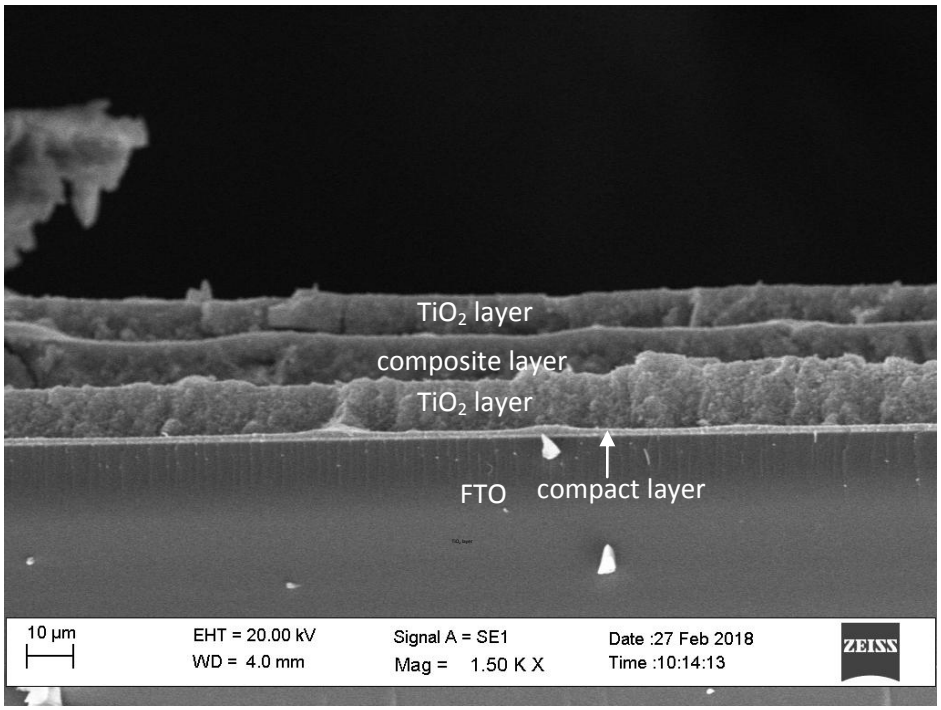

Fig.3 (a): SEM cross section image of TiO_2 photoanode of the tri-layered structure; P25/P25+Ag NW+TiO_2 NF/P25 formed on FTO/P-90 compact layer correspond to the DSSC showing the best photovoltaic performance. The composite middle layer consists of the optimized composition of P25+Ag NW+TiO_2 NF.

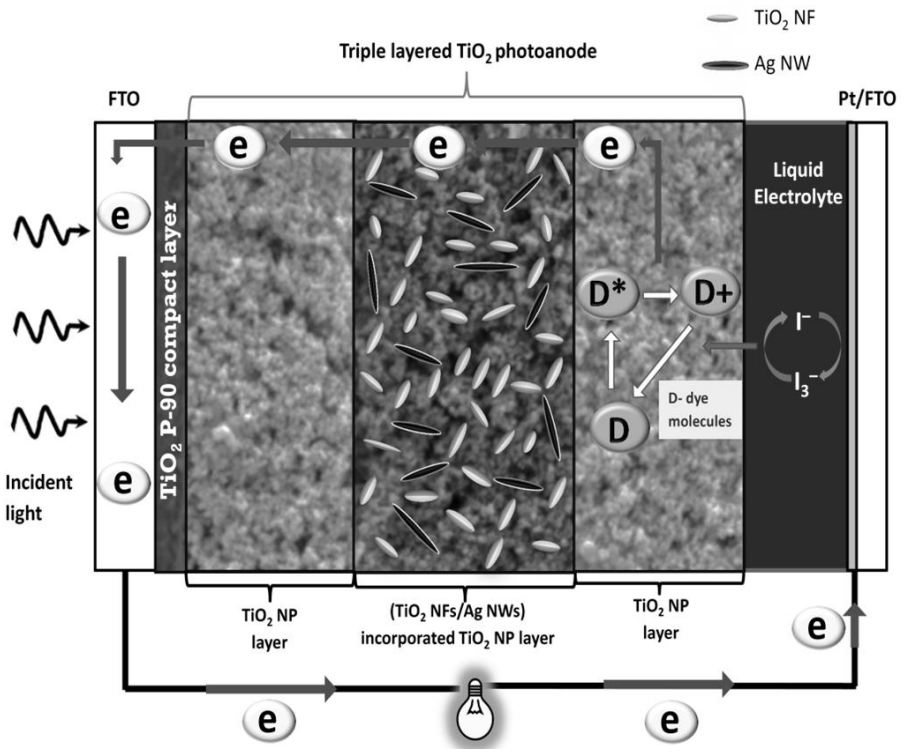

Fig. 3(b) : A schematic diagram of the DSSC with the tri-layer photoanode (d) P25/P25+Ag NW+TiO_2 NF/P25.

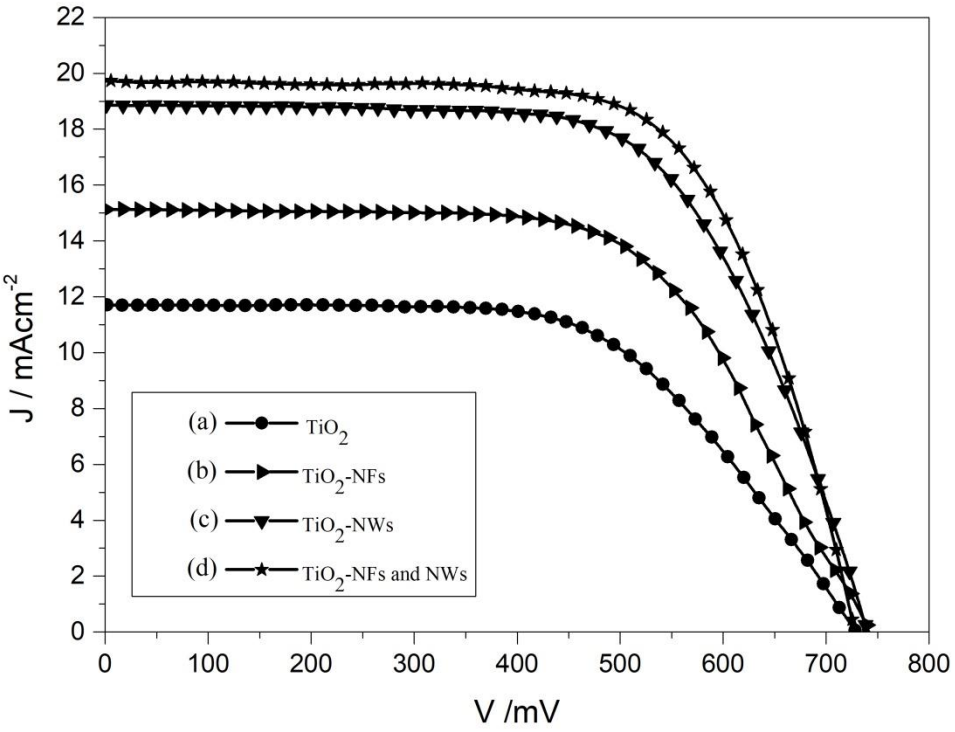

Fig 4: *J-V* curves taken for DSSCs with tri-layer photoanodes (a) P25NP/P25NP/P25NP tri-layer with TiO_2 P25NP as the middle layer, (b) P25NP/(P25NP+TiO_2 NFs)/P25NP, with the P25NP mixed with TiO_2 NF as the middle layer, (c) P25NP/(P25NP+AgNWs)/P25NP, with the P25NP mixed with AgNW as the middle layer and (d) P25NP/(P25 +Ag NWs + TiO_2 NFs) /P25NP, with the P25NP mixed with TiO_2 NFs and Ag NWs as the middle layer.

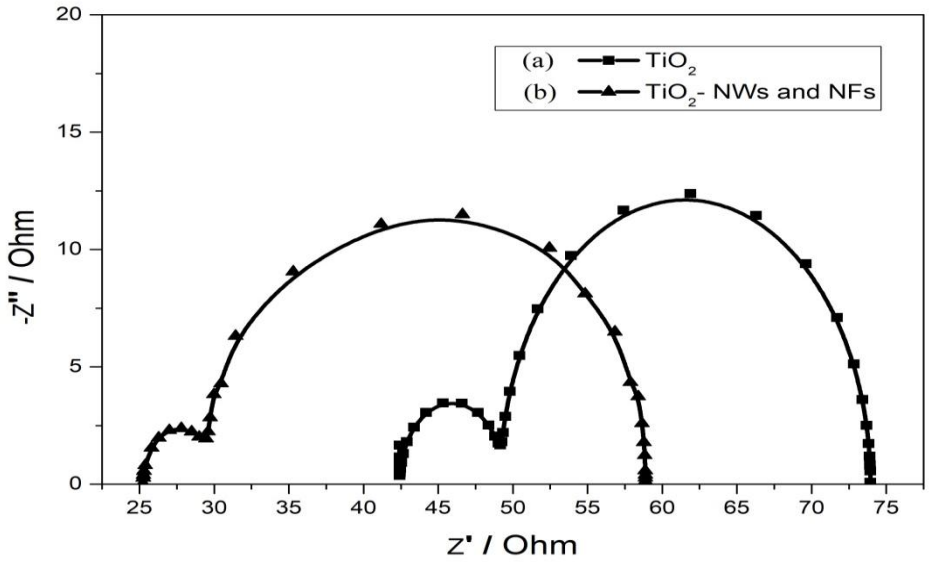

Fig.5 Impedance plots taken for the DSSCs with photoanodes with configurations (a) (P25/P25/P25) and (b) (P25/P25+Ag NW+TiO_2 NF/P25) in the frequency range 11×10^{-2} to 1×10^{6} Hz.

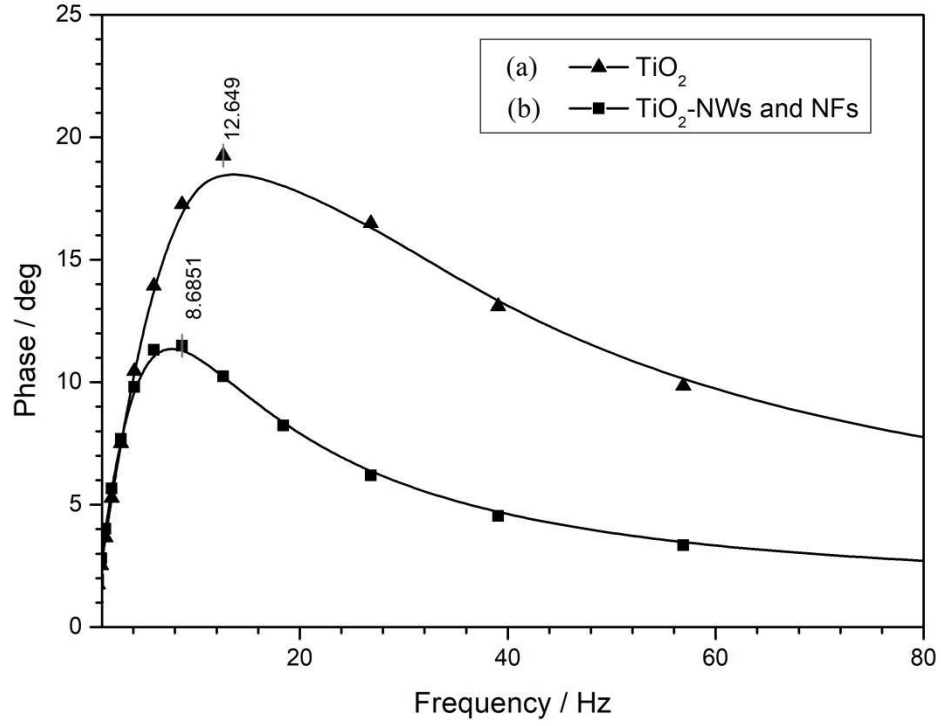

Fig.6. Bode phase plots taken for the DSSCs with photoanodes with configurations (a) (P25/P25/P25) and (b) (P25/P25+Ag NW+TiO_2 NF/P25) in the frequency range 11×10^{-2} to 1×10^{6} Hz.

GRAPHICAL ABSTRACT for On-line version

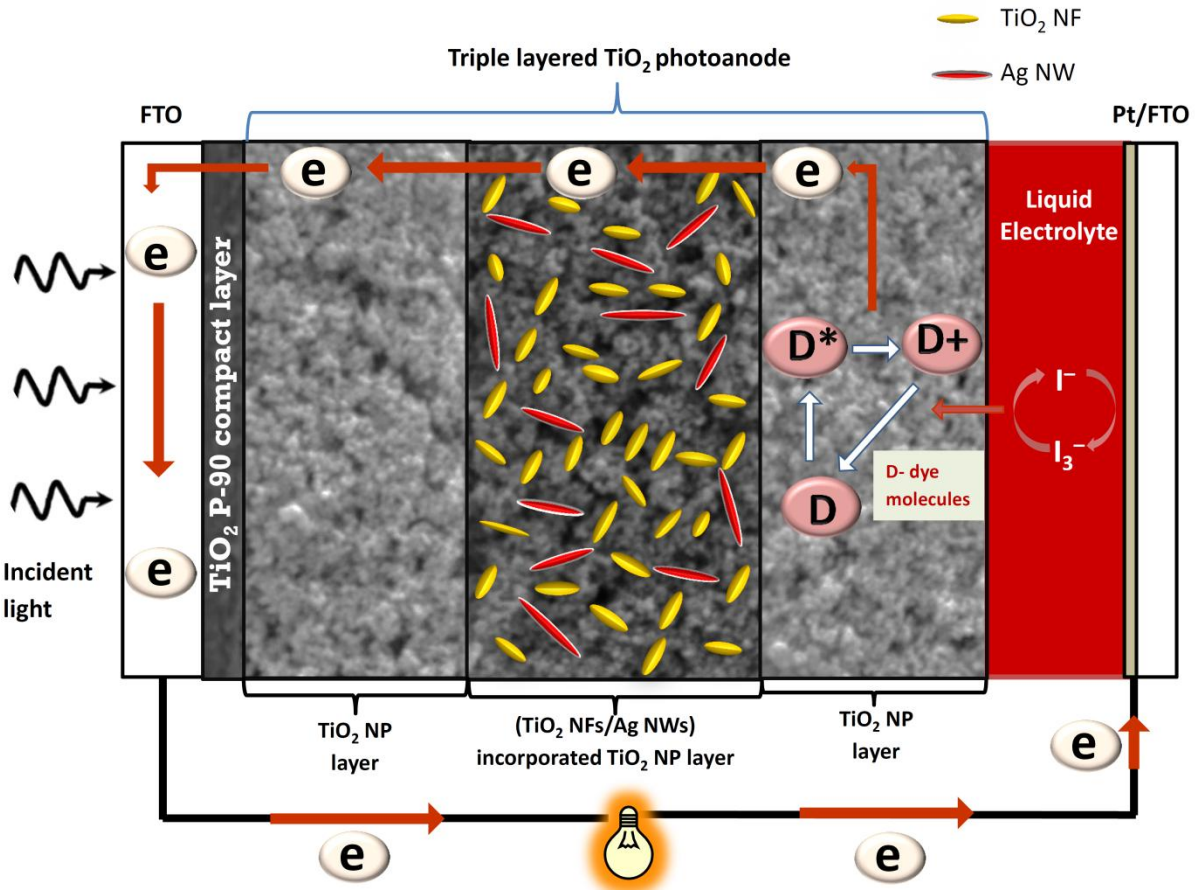

Research Highlights

- A composite multilayered layered TiO_2 photoanode was fabricated and tested in dye solar cells
- The middle layer is made of TiO_2 25P mixed with silver nanowires and TiO_2 nanofibres
- Power conversion efficiency of 9.74% and short circuit current density 19.8 mA cm^{-2} were achieved
- This is an efficiency enhancement of 45.6 % compared to a solar cell with three layers of TiO_2 25P of same thickness
- Increased efficiency is attributed to plasmon enhanced photocurrent and scattering enhanced light absorption.